Journal of Atmospheric and Solar-Terrestrial Physics 70 (2008) 1497–1511

Contents lists available at ScienceDirect

Journal of Atmospheric and Solar-Terrestrial Physics

journal homepage: www.elsevier.com/locate/jastp

What are the influences of solar eclipses on the equatorial electrojet?

A.T. Tomás [a,*], H. Lühr [a], M. Rother [a], C. Manoj [b,1], N. Olsen [c], S. Watari [d]

[a] GeoForschungsZentrum Potsdam, Telegrafenberg, D-14473 Potsdam, Germany
[b] National Geophysical Research Institute, Uppal Road, Hyderabad 500 007, India
[c] Danish National Space Center, Juliane Maries vej 30, DK-2100 Copenhagen, Denmark
[d] National Institute of Information and Communications Technology, Japan

ARTICLE INFO

Article history:
Received 8 August 2007
Received in revised form
2 May 2008
Accepted 17 May 2008
Available online 7 July 2008

Keywords:
Equatorial ionosphere
Solar eclipse
Equatorial electrojet response
Ionospheric disturbances

ABSTRACT

The response of the equatorial electrojet (EEJ) to solar eclipses is studied in this work. We analyzed the magnetic field measurements obtained by three satellites, CHAMP, SAC-C and Ørsted and correlated them with ground-based observations during the eclipses. The observations show a local weakening of the EEJ after the shadow passed the dip equator. The size of the effect is, however, comparable with the day-to-day variability. In four out of five events we found the formation of a counter electrojet in the wake of the eclipse. We propose that the depression of the EEJ during an eclipse favors the formation of a counter electrojet.

1. Introduction

Solar eclipses can be considered as a large-scale experiment performed by nature. In particular, the ionosphere is known to experience significant changes in response to the blocking of the sun. Although quite a number of studies have been published on solar eclipses effects (Beynon and Brown, 1956; Salah et al., 1986; Cheng et al., 1992; Korte et al., 2001) there is still no consensus on the typical response of the current systems. The infrequent occurrence of solar eclipses and the sparse distribution of suitable observatories have largely hampered the clear identification of cause and effect relations. In many cases the day-to-day variabilities have the same amplitude as the effects observed during the eclipses.

Among the various ionospheric effects reported, the reduction of the E region electron density is one of the most frequently confirmed (Rishbeth, 2000; Korte et al., 2001). At this low altitude ionospheric layer the amount of charged particles is closely related to the amount of incident short wavelength radiation. As a direct consequence, if the incident radiation is reduced, a proportional reduction of the ionospheric conductivity is expected and with that weaker ionospheric currents. Interestingly, Korte et al. (2001) could not confirm this chain of relations at mid-latitudes. Although the E region electron density was markedly reduced, no significant change in S_q current strength was detected.

It has been repeatedly claimed that the solar eclipse effects should be clearer at the dip equator since this is where there is no possibility for the ionospheric currents to be rerouted through the conjugate ionosphere.

In this study we focus on the effects an eclipse may have on the equatorial electrojet (EEJ). This current is confined to a narrow latitudinal strip centered on the dip equator, where the conductivity is greatly enhanced. For further details about the EEJ the reader may be referred to Forbes (1981) and Onwumechili (1997). So far the published studies about the effect on the EEJ have been limited to a few case studies (Beynon and Brown, 1956; Cheng et al., 1992; Tomás et al., 2007). Here we try to

* Corresponding author. Tel.: +49 331 2881444.
E-mail address: tomas@gfz-potsdam.de (A.T. Tomás).
[1] Current address: National Geophysical Data Center, Boulder, CO 80305-3328, USA.

1364-6826/$ - see front matter © 2008 Elsevier Ltd. All rights reserved.
doi:10.1016/j.jastp.2008.05.009

investigate a larger sample number using a common approach in order to identify the eclipse related features.

It is expected that the EEJ intensity will be reduced within the shadow zone. During times of weak electrojets frequently a reversal of the current flow, the so called counter electrojet (CEJ), is observed (Rastogi, 1974). Therefore, solar eclipses may act as a trigger for a CEJ.

The few studies done on the CEJ phenomena have not allowed to fully explain the mechanism behind it (Rastogi, 1974; Mayaud, 1977). Many points remain unclear. Mayaud (1977) suggests two possible sources for the CEJ. The first possibility is based on a connection between the S_q vortices and the EEJ. In some cases negative values of the horizontal magnetic component (H) were observed at the equator (the signature of the CEJ), and positive values of the vertical magnetic component (Z) were observed at higher northern latitudes, indicating that both components are subject to the same anomaly. From the present perspective we would relate these events to the direct penetration of an westward electric field from high latitudes, affecting all latitudes simultaneously.

The other possibility mentioned by Mayaud (1977) concerns the coexistence of an eastward (EEJ) current and a westward (probably higher) current. If the layer where the background currents flow is twice as thick as the layer where the electrojet flows, any small variation in altitude of the region where a CEJ occurs, would cause rapid variations in its intensity. Thus a weakening of the EEJ could result in a negative deflection of the component on the ground.

According to Rastogi (1974) there are certain conditions favoring the occurrences of a CEJ. Preferable local times are the morning and evening hours. In terms of seasonal dependence, the morning CEJ is reported to be more frequent during the equinoxes than June solstices. The afternoon CEJ is claimed to have an occurrence maximum around June solstice and a secondary peak at December solstice. This seasonal dependence is, however, controversially discussed (Reddy, 1989). For the solar cycle dependence Rastogi (1974) observed an anti-correlation between the number of sun spots and the number of CEJs, in particular for the afternoon events, less clear for the morning events. A lunar dependence of the CEJ was mentioned by Rastogi (1989) indicating a greater occurrence at new and full moon.

A combination of ground-based with satellite observations may help to better understand the changes in current systems during a solar eclipse. This includes the mechanisms that are behind a CEJ. The merged data set helps, in particular, to obtain a much improved view of the variations, both in time and space. Never before has such a comprehensive study on solar eclipse effects been performed.

In order to address this question, we used the data collected during solar eclipses of recent years by the three satellites, CHAMP, SAC-C and Ørsted, as well as ground-based magnetometers whenever suitably located.

The attempts to study equatorial solar eclipses in the decade from 1990 to 2000 were particularly unsatisfactory. Only five eclipses were simultaneously equatorial and in the vicinity of ground-based stations. Unfortunately, due to the absence of data (in four of those cases) and low quality data (in the other case), it was not possible to analyze these events. This illustrates the difficulty of the topic addressed and reiterates the importance of including satellite data, with a higher spatial coverage, to obtain a more detailed picture of the eclipse effects.

The German satellite CHAllenging Minisatellite Payload (CHAMP) was launched on 15 July 2000 and circles the Earth at an initial altitude of about 400 km on a nearly circular orbit with an inclination of 87.25° (Reigber et al., 2002). The high inclination of the orbit allows for a nearly complete latitudinal coverage. Furthermore, the fact that the orbit is near circular increases temporal and spatial resolution. CHAMP also provides local measurements of electron density and temperature. The studies of thermospheric dynamics and the response of the neutral atmosphere to a solar eclipse can be performed from the analysis of accelerometer measurements on board CHAMP. High precision magnetic field measurements can be employed for investigating the response of ionospheric currents.

The Argentinian Satelite de Aplicanciones Cientificas-C (SAC-C) satellite was launched on 21 November 2000. The spacecraft circles the Earth on a near polar orbit at about 700 km altitude with a 98° inclination. SAC-C is in a sun-synchronous orbit, crossing the equator at 10:30 and 22:30 local time (LT). The instruments on board of importance to this work are the magnetometers, since they have been providing continuous scalar magnetic field measurements until December 2004.

The Danish Ørsted satellite was launched on 23 February 1999 in a near polar orbit with an inclination of 98°. The altitude of the satellite varies between 640 km at perigee and 880 km at apogee. The principal aim of the mission is to make an accurate map of the Earth's magnetic field, therefore high quality magnetic field measurements from two magnetometers are available (Neubert et al., 2001).

2. Observations

In this study we have analyzed a set of eclipses occurring in the time period from 2001 to end of 2006. With the purpose of studying EEJ changes during solar eclipses, only those which crossed the dip equator or passed sufficiently close to the dip equator were taken into account. The 4 eclipses analyzed occurred on 14 December 2001 (event A), 10 June 2002 (event B), 3 October 2005 (event C) and 29 March 2006 (event D). Table 1 indicates the eclipse initial and final coordinates (in terms of Universal Time (UT), geographic longitude and latitude), as well as the location of the dip equator crossing (or closest approach). The indicated geographic coordinates correspond to the center line of the eclipse at the Earth's surface. Information pertaining to the solar eclipses was obtained from the NASA Solar Eclipse web page (http://sunearth.gsfc.nasa.gov/eclipse/eclipse.html).

The location of the eclipses as well as the CHAMP passes analyzed in this paper are shown in Fig. 1.

Table 1
Eclipse coordinates for the initial– final points, and location of the dip equator crossing by the eclipse

Eclipse	Date	Initial–final			Dip equator crossing		
		UT	Geo. Lat.	Geo. Long.	UT	Geo. Lat.	Geo. Long.
A	14 December 01	19:15–22:30	22.33 N–8.52 N	168.90 W–89.20 W	21:00	0.12 N	128.61 W
B	10 June 02	21:55–01:30	3.56 N–25.85 N	125.68 E–118.93 W	22:05	11.73 N	135.68 E
C	3 October 05	08:45–12:20	46.43 N–9.85 S	24.47 W–77.08 E	10:45	9.65 N	31.30 E
D	29 March 06	08:40–11:45	4.15 S–51.75 N	22.12 W–82.15 E	09:30	11.23 N	5.73 E

Indicated are: Universal time (UT, in h), geographic latitude and longitude (in degrees).

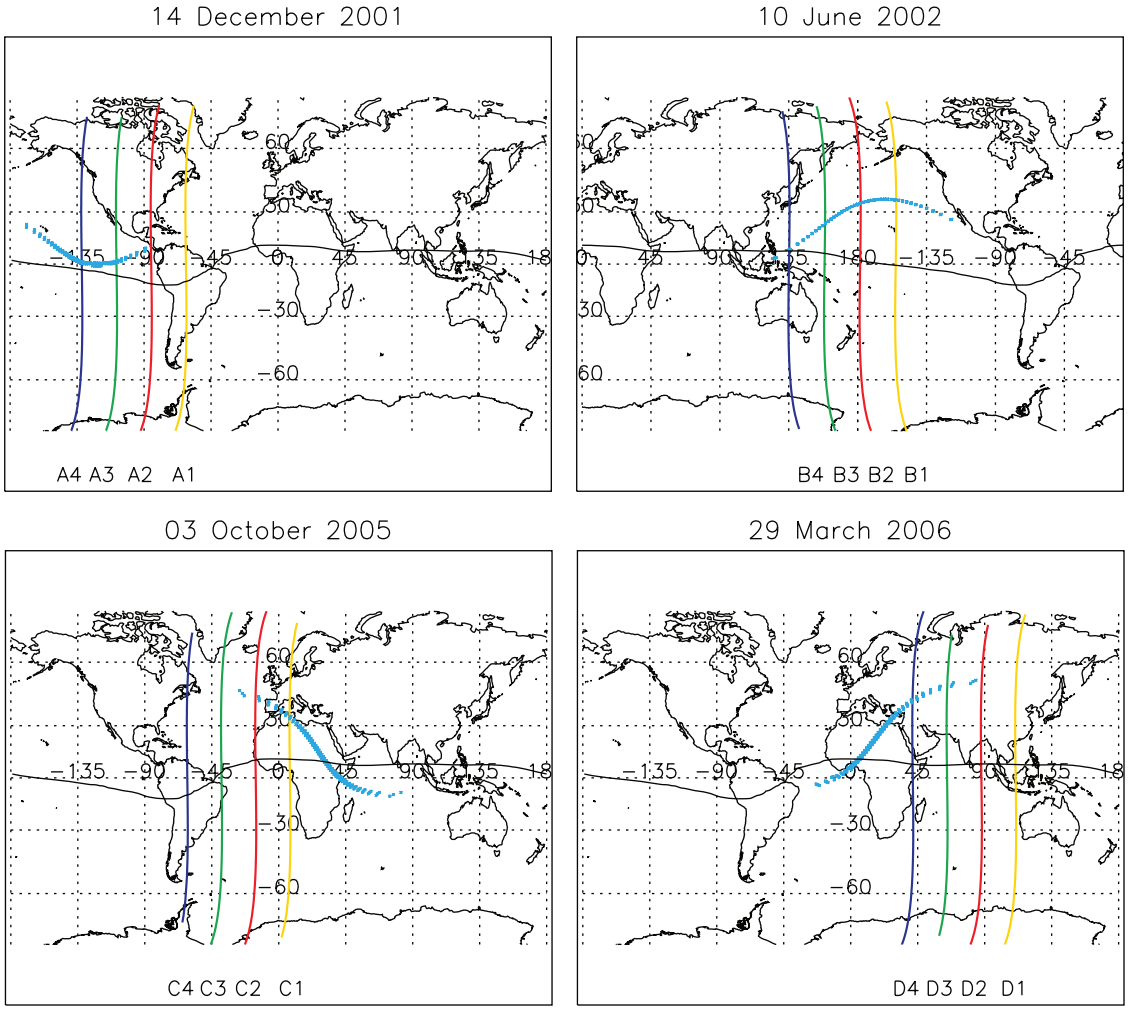

Fig. 1. World map projection for the four eclipses, showing the path of the umbral/antumbral shadow (cyan), the CHAMP passes considered and the latitude of the magnetic equator (solid line). The time for each pass (accordingly labeled) can be found in Table 2.

The labeling of the different passes indicates the eclipse event (letter) and the pass (number) which correspond to a certain UT interval. The color code, as well as the labels shown here, will be consistently used throughout the work. Table 2 indicates the location, in terms of Universal Time (h) and Geographic longitude (degrees) of the dip equator crossing in each pass, for the three satellites considered. The LT, which remains constant within each event, is also indicated.

In the following sections we discuss each of these eclipses in terms of the EEJ observations made by CHAMP, Ørsted, SAC-C (until 2004) and ground-based observations. For the three satellites the EEJ current distribution is obtained from the scalar magnetic field measurements.

Table 2
Dip equator crossings of CHAMP, SAC-C and Ørsted during the analyzed four passes (for each eclipse)

Eclipse	Date	Pass 1		Pass 2		Pass 3		Pass 4		LT
		UT	Geo. Long.	UT	Geo. Long.	UT	Geo. Long.	UT	Geo. Long.	
CHAMP passes										
A	14 December 01	19:36	61.69 W	21:54	85.00 W	22:40	108.40 W	00:14	131.79 W	15:26
B	10 June 02	21:34	155.15 W	23:05	178.34 W	00:37	158.49 E	02:09	135.27 E	11:12
C	03 October 05	09:19	15.63 W	10:49	38.50 W	12:17	61.29 W	13:49	84.25 W	08:12
D	29 March 06	08:33	110.69 E	10:05	87.65 E	11:37	64.65 E	13:08	41.57 E	15:54
SAC-C passes										
A	14 December 01	18:54	127.40 W	20:32	151.43 W	22:10	175.44 W	23:48	160.70 E	10:30
B	10 June 02	20:21	148.31 W	21:59	172.35 W	23:37	163.81 E	01:15	139.51 E	10:30
Ørsted passes										
A	14 December 01	18:52	119.26 W	20:32	143.58 W	22:10	167.97 W	23:49	167.80 E	11:00
B	10 June 02	20:56	171.09 E	22:35	146.68 E	24:15	121.76 E	01:55	96.85 E	08:18
C	03 October 05	07:59	95.42 E	09:39	70.37 E	11:17	45.42 E	12:58	20.90 E	14:20
D	29 March 06	07:49	58.69 E	09:29	33.98 E	11:08	9.35 E	12:48	15.81 W	11:44

Indicated are: Universal time (UT, in h), longitude (in degrees) and local time (LT, in hours).

Table 3
Geographic and geomagnetic conditions of the ground-based stations used

Station	Geo. Lat	Geo. Long	Geo. Lat	Geo. Long.	Local time
YAP–Yap	9.3 N	138.5 E	0.3	209.0	UT + 9.2 h
KDU–Kakadu	12.69 S	132.47 E	21.99	205.44	UT + 8.8 h
AAE–Addis Ababa	9.02 N	38.77 E	5.27	111.57	UT + 2.6 h
QSB–Qsaybeh	33.87 N	35.64 E	30.23	113.37	UT + 2.4 h

Since the magnetic field data contain the sum of various contributions, we have to remove the other parts in order to isolate the effects of the EEJ.

In the case of CHAMP, the magnetic field model used for the subtraction is Potsdam Magnetic Model of the Earth (POMME 3) (Maus et al., 2006). For both Ørsted and SAC-C the magnetic field model used for subtraction is the CHAOS model (Olsen et al., 2006). These models include a correction for the effect of the magnetospheric ring-current. To further remove the influence of large-scale ionospheric currents, such as S_q, we fitted and subtracted a degree 5 polynomial from the residuals for magnetic latitudes equatorward of 58°. In this fitting procedure the vicinity of the dip equator (±14°) was omitted in order to avoid a feedback of the EEJ signature on the result.

The ground-based observations are obtained from the magnetic observatory closest to the eclipse path, and the corresponding reference station. The detailed coordinates of the observatories used are given in Table 3. In order to characterize the strength of the EEJ we derived an EEJ index in the following way: we took the measured horizontal field component, from both stations and subtracted a baseline (i.e. the value around midnight) from each set. The EEJ index was then calculated by subtracting the reduced H components of the reference station from that of the EEJ observatory.

We start by presenting the observations of the 10 June 2002 eclipse since for this event a good coverage from the three satellites, as well as from ground-based data is available.

2.1. A case study—10 June 2002

The solar eclipse on 10 June 2002 (event B) was an annular solar eclipse, visible mostly in the northern Pacific region. The eclipse started at 21:55 UT and ended at 01:30 UT of the following day. The dip equator crossing occurred early, at 22:05 UT. Detailed coordinates are given in Table 1. On the 10th of June the geomagnetic activity index (K_p) was 3− from 21:00 to 24:00 UT and 2+ from 24:00 to 03:00 UT, indicating moderate activity. The solar flux index (F10.7) was 151.6 on 10 and 147.8 on 11 June, indicating moderate solar activity.

Fig. 2 shows the magnetic variations observed by CHAMP (first panel), SAC-C (second panel) and Ørsted (third panel). The four passes analyzed occurred before, during and after the indicated eclipse period. The local times of the three satellites in the above order are, respectively, 11:12, 10:30 and 08:18 LT.

The CHAMP profiles for the first two passes (B1 and B2) show the typical magnetic field profile of the EEJ, a negative deflection peaking at the dip-equator accompanied by positive shoulders north and south of it. In this case the peak-to-peak variations are not very pronounced, of the order of 7 nT (for B1) and 15 nT (for B2). The last two

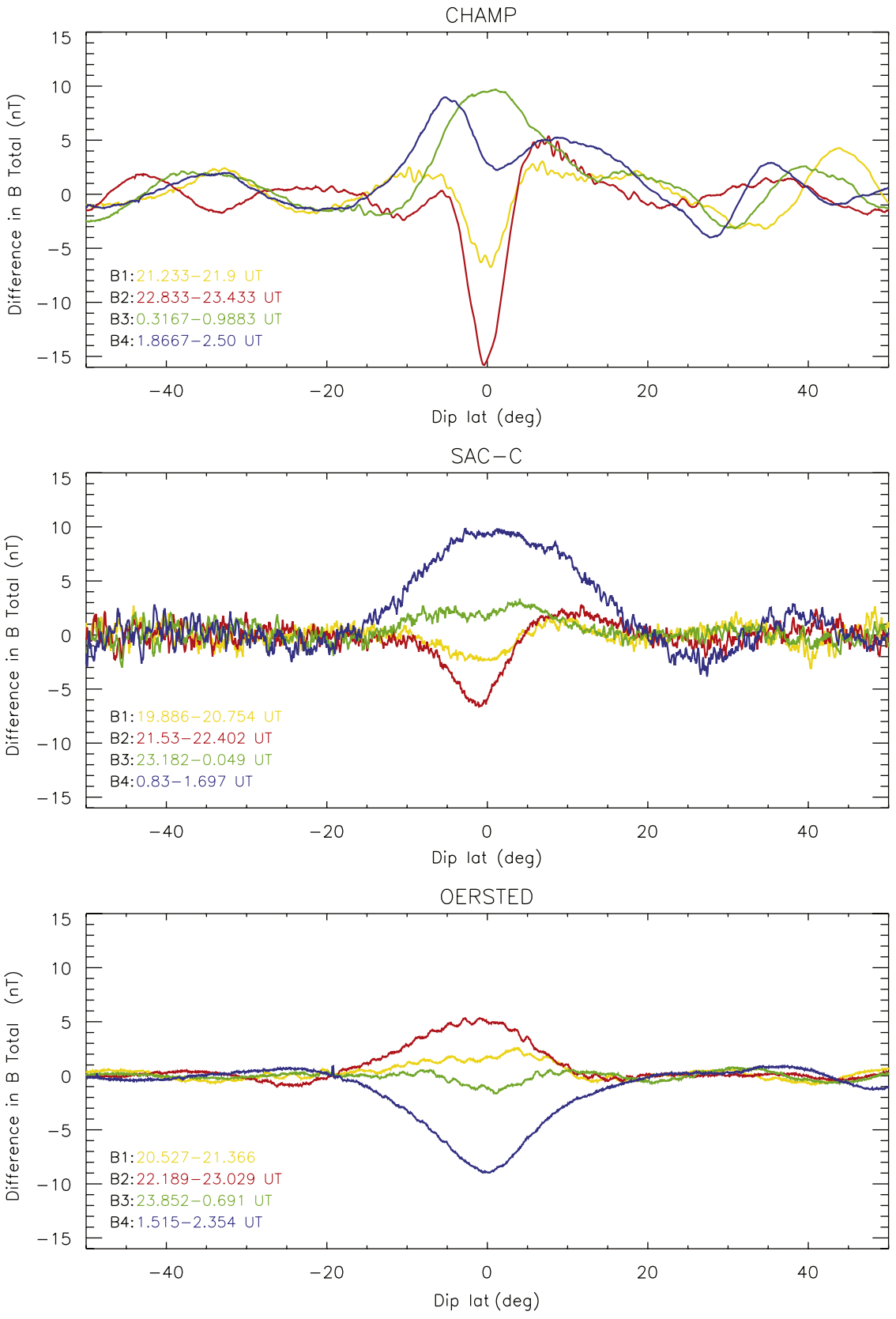

Fig. 2. 10 June 2002: Latitudinal variation of the total magnetic field component for CHAMP, SAC-C and Ørsted. Time of the different passes is indicated by color.

passes clearly show a perturbed EEJ profile. For the B3 pass (green) a reversal of the EEJ profile, i.e. a CEJ, is clearly seen. The observed positive peak is much broader in latitude than the normal EEJ profile. On the following B4 pass the profile seems to indicate a superposition of the two effects, with the positive values around the dip equator indicating a CEJ, but with the shape of the profile returning to that of a typical EEJ profile. The crossing of the dip equator during the B3 pass occurs 2.5 h after the eclipse crossed the dip equator (see Tables 1 and 2).

The SAC-C profiles show the CEJ feature during the B4 pass (blue). The previous pass, B3, shows already a disturbed profile, evolving towards a CEJ. The earlier passes (B1 and B2) show the EEJ profile. The dip equator crossing of the B4 pass occurs 3 h after the eclipse crossing.

The Ørsted profiles already start with a disturbed EEJ profile (B1 pass), which evolves into the CEJ profile on the consecutive pass (B2). The last two passes (B3 and B4) show a return to the EEJ profile. The absence in the profiles of the typical flanks north and south of the dip equator is due to the higher altitude of the latter two satellites, when compared to CHAMP.

Both SAC-C and Ørsted show CEJ profiles similar to that of CHAMP with the positive peak being broader in latitude.

The EEJ ground-based station considered for this eclipse was YAP (in the Pacific Ocean) and the reference station KDU (in Australia). From the horizontal component of the magnetic field, we calculated the EEJ index (as defined in Section 2). One should note that the more appropriate reference station for YAP, would be BIK (latitude: 1.08°S, longitude: 136.05°E), but unfortunately no measurements were available for 10 June 2002. For this reason we have chosen the KDU reference station despite its distance to YAP (∼20° southward).

Fig. 3 shows in the upper panel the EEJ index for the period from 9 to 14 June 2002. The vertical dotted lines indicate the eclipse period. On the eclipse day the EEJ is largely depressed with many negative excursions of the EEJ index. The middle panel shows the Dst index for the same time period and the lower panel displays the variation of the EEJ index around the eclipse period. Also indicated are the times of satellite dip equator crossings in this time period. In red is the Ørsted pass B2 (20:56 UT), in green are the CHAMP pass B3 (00:37 UT), SAC-C pass B3 (23:37 UT) and Ørsted pass B3 (00:15 UT) and in blue are the CHAMP pass B4 (02:09 UT) and SAC-C pass B4 (01:15 UT). On Ørsted pass B2 a clear CEJ is observed at satellite height while the EEJ index at YAP is close to zero. At the time of the CHAMP B3 crossing the measured EEJ index is clearly negative, indicating a reversal of the horizontal current, i.e. a CEJ, which is also detected by CHAMP, 20° eastward of YAP.

However, by looking at the EEJ index over the five day period, one can see an irregular EEJ variation starting around 10 UT on the 10th and which lasts until 12 June. By comparing it with the Dst index variation it becomes clear that it coincides with the onset of a magnetic storm, which affects the following two days and therefore also the eclipse period. The intensity of the EEJ is largely suppressed on 11 and 12 June probably by the action of the disturbance dynamo. We thus cannot exclude that the observed CEJs at the time of the eclipse are a result of the perturbations caused by the magnetic storm.

2.2. Further examples

2.2.1. 14 December 2001

The solar eclipse on 14 December 2001 was an annular eclipse, visible in the northern hemisphere, over the western Pacific Ocean. The eclipse started at 19:15 UT and ended at 22:30 UT (see Table 1). The eclipse did not cross the dip equator but the closest approach was within 4° latitude of the dip equator, sufficiently close to be considered in our analysis. During the eclipse the K_p index was 2 from 18:00 to 21:00 UT, indicating low activity. The solar flux index on this day was 216.6 indicating high solar activity.

Fig. 4 shows the magnetic variations observed by the three satellites in the same format as Fig. 2.

The CHAMP profiles for the first two passes (A1 and A2) show the typical profile of the EEJ, a negative deflection peaking at the dip equator accompanied by positive shoulders north and south of it. In this case the peak-to-peak variations are not very pronounced and of the order of 10 nT. The last two passes (A3 and A4) clearly show a reversal of the EEJ profile, i.e. a CEJ. The observed positive peak is much broader in latitude than the normal EEJ profile. The A3 pass (green) crosses the dip equator 1.5 h after the eclipse. The A4 pass (blue) crosses the dip equator approximately 3 h after the eclipse had its closest approach to the dip equator.

The profiles of SAC-C and Ørsted for the four passes show the typical profile of the EEJ, with peak-to-peak variations up to 20 nT. During this event Ørsted and SAC-C cross the dip equator practically at the same times and the orbits are separated only by about 8° in longitude. Therefore their samples are almost identical, as is also evident from Fig. 4. This reduces the number of independent observations. SAC-C observes an amplitude reduction of the order of 50% in the A2 pass (compared to A1), which becomes more pronounced in the following pass (A3), with the minimum value being close to zero. The last pass (A4) shows a return towards the initial situation. Subsequent passes (not presented here) show a further return to the initial situation.

As mentioned in Section 1, abnormal variations of the vertical magnetic field component, Z, have been observed simultaneously on the ground during a CEJ. Since in this case we had a clear EEJ in the first two CHAMP passes (A1 and A2) and a clear CEJ in the last two passes (A3 and A4), we analyzed the Z component to see if such a change was also present. Fig. 5 shows that this is indeed the case. Passes A1 and A2 exhibit the normal variation of the Z component, while passes A3 and A4 show a reversed profile.

Due to the location of the eclipse over the Pacific Ocean, it was not possible to obtain ground-based measurements. The nearest observatory, Huancayo

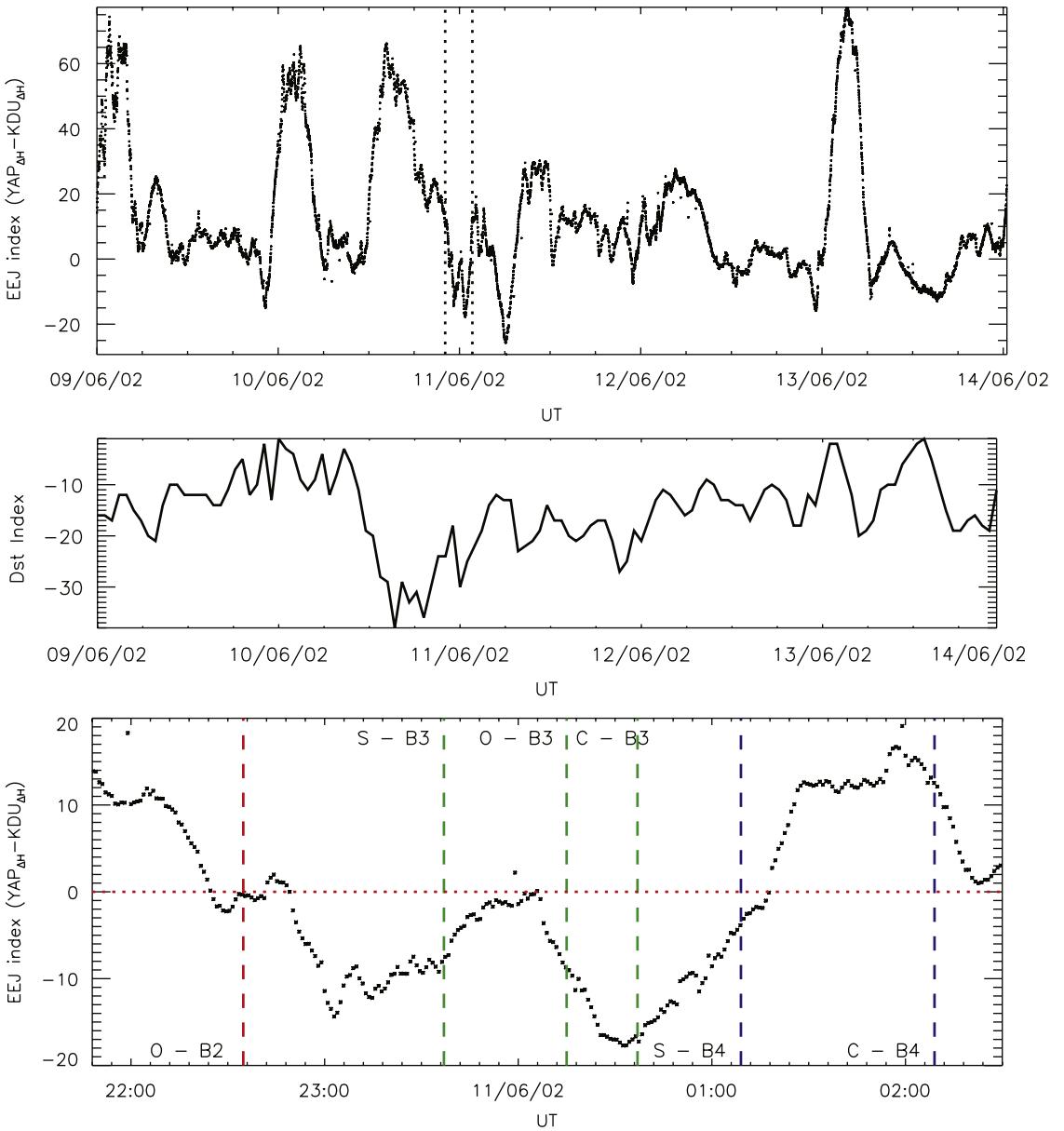

Fig. 3. Upper panel: EEJ index for the 9–13 June 2002 period obtained from the YAP/KDU stations. Dotted lines indicate the eclipse period. Middle Panel: Dst index for the same time period. Lower panel: EEJ index around the eclipse time. Dashed lines indicate the Ørsted (O) B2 pass (in red), the B3 passes (in green) for CHAMP (C), SAC-C (S) and Ørsted, and the B4 passes (in blue) for CHAMP and SAC-C.

(12.04°S latitude, 75.32°W longitude), showed no indication of a CEJ.

2.2.2. 3 October 2005

The solar eclipse on 3 October 2005 was an annular solar eclipse, crossing the Iberian peninsula into the African continent. The eclipse started at 08:45 UT and ended at 12:20 UT. The dip equator crossing occurred at 10:45 UT. Geomagnetic conditions during the eclipse indicated low activity, with K_p being 2 between 06:00 and 09:00 UT, and 2 from 09:00 to 12:00 UT. The solar activity was low, with a F10.7 of 74.3.

Fig. 6 shows the magnetic variations observed by CHAMP and Ørsted. On the upper panel, CHAMP observations indicate during the first two passes (C1 and C2) a EEJ profile with peak-to-peak variations of 10 nT. The two later passes exhibit a perturbed profile shape, a CEJ profile during pass C3. This pass occurred at 12:17 UT, i.e. 1.5 h after the dip equator crossing of the eclipse. The following pass (C4) indicates a superposition of both CEJ and EEJ signatures, similar to the one observed on the B4 pass (10 June 2002 eclipse). The Ørsted observations show a normal EEJ profile on the C1 pass, but a perturbed situation in the following passes, showing the evolution

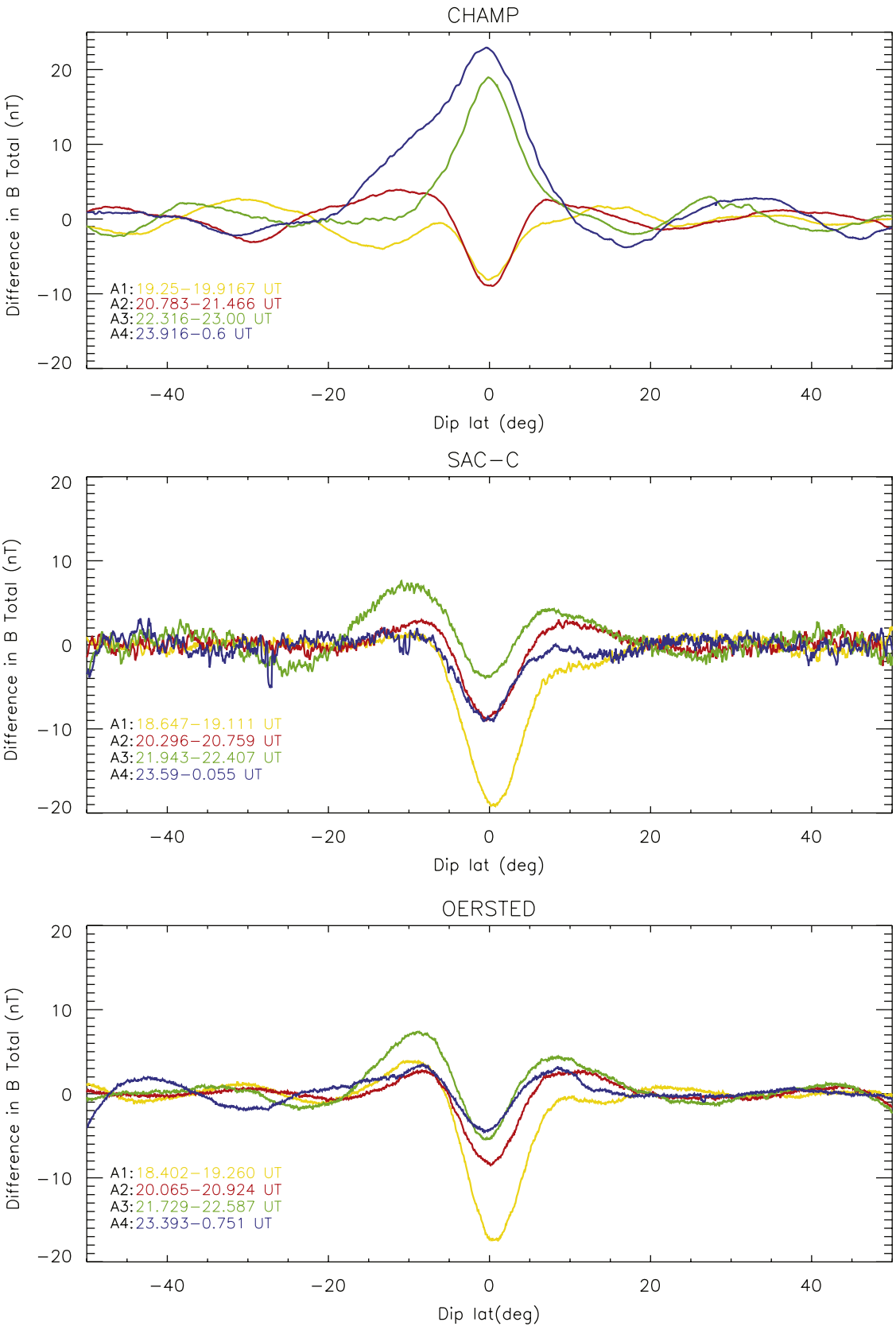

Fig. 4. 14 December 2001: Latitudinal variation of the total magnetic field component for CHAMP, SAC-C and Ørsted. Time of the different passes is indicated by color.

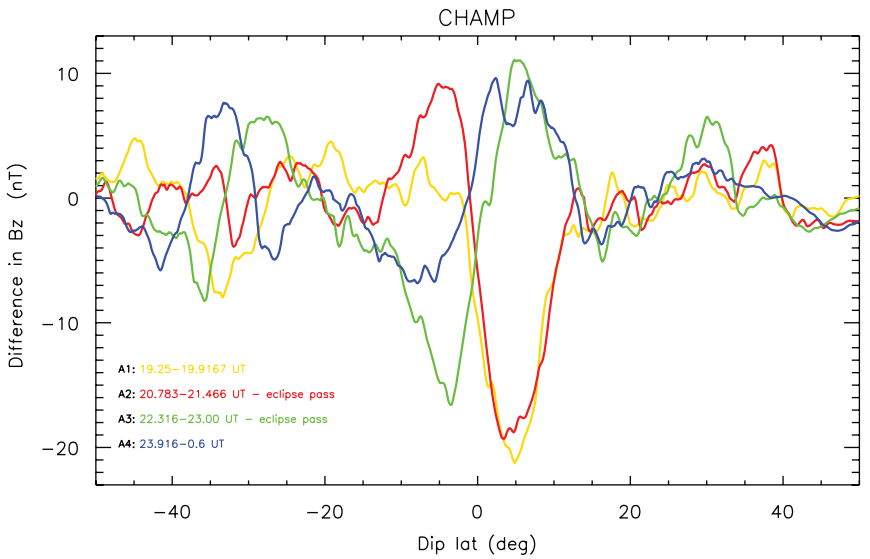

Fig. 5. 14 December 2001: Latitudinal variation of the B_z magnetic field component for CHAMP. Time of the different passes is indicated by color.

towards the CEJ profile (on C4). The C4 pass occurs at 12:58 UT, approximately 2 h after the eclipse crossed the dip equator.

The EEJ index could also be calculated from ground-based observations. The considered stations were AAE and the reference station QSB, located at 33.87° latitude. Fig. 7 shows the EEJ index for the period between 30 September and 7 October (upper panel), and the EEJ index during the eclipse (lower panel). Due to the proximity of the dip equator crossing of the eclipse (7.5° in longitude) this ground record provides valuable information about the eclipse effect on the electrojet. The somewhat reduced peak EEJ index on the eclipse day may well be related to the shadow effect. Visible towards the end of the eclipse is the development of a CEJ. However on the 1st of October, two days before the eclipse, a CEJ occurring at the same universal time (around 12 UT) is also seen. The clear CEJs on 5 and 6 October occur in the morning period and are therefore not unusual. Also Somayajulu et al. (1993) reported about the preference of CEJs to occur at certain reoccurrence periods. From Fig. 7, lower panel, it can be seen that the CEJ at the time of the eclipse lasted from 11:15 to 13:25 UT. Lowest magnetic field readings were obtained at a local time around 14:30. The CHAMP dip equator crossing on pass C3 (dashed line) is close to the time when the EEJ index has its negative peak, but at a rather different longitude (cf. Fig. 1).

2.2.3. 29 March 2006

The solar eclipse of 29 March 2006 was a total solar eclipse visible from West Africa through Central Asia. The eclipse started at 08:40 UT and ended at 11:45 UT. The dip equator crossing occurred at 09:30 UT. The K_p index was 1 from 06:00 to 09:00 UT and 1 from 09:00 to 12:00 UT, indicating calm geomagnetic conditions. On this day, the F10.7 index was 81.7, indicating low solar activity.

In this particular example the satellite residuals were fitted by a seventh degree polynomial due to high oscillations on the Ørsted magnetic field data, in the region around 40°S. The magnetic variations for the analyzed CHAMP passes can be seen in the upper panel of Fig. 8. Both eclipse passes, D2 and D3, show the perturbed shape, as we observed it in the CHAMP B4 and C4 passes. In this particular case, D1 and D4 were closer to the typical EEJ profile. A clear CEJ profile is not observed. The Ørsted observations show the magnetic variations changing from a typical EEJ profile in the first three passes, to an asymmetric CEJ profile on the last pass (D4).

The EEJ index calculated for this event, based on the AAE and QSB stations, can be seen in Fig. 9. The same format as in the previous figures is used, with the upper panel showing the EEJ index for the time period from 26 March to 2 April 2006. During this event the eclipse crossed the dip equator about 33° in longitude further west. As expected, the effect of the EEJ at AAE is much less than during the previous event. For the time of the eclipse (lower panel) one can see that the index remains positive and no CEJ can be associated with the eclipse. Two afternoon CEJs occurring around 12–13 UT are visible on 26 March and on 1 April. It is interesting to note that Ørsted's pass D2, indicated by the dashed red line, occurs at 33.98°E longitude, which is quite close to the longitude of the geomagnetic observatory AAE (38.77°E). During this pass Ørsted observes the typical EEJ profile, and the EEJ index at AAE is around its maximum for the corresponding time (09:29 UT), indicating a good agreement between ground and satellite observations.

3. Discussion

In order to study the effects of solar eclipses on the EEJ, we have analyzed the observations of the EEJ variation at the times of the four solar eclipses. Our study revealed the occurrence of a CEJ mostly 1–3 h after the eclipse crossed the dip equator.

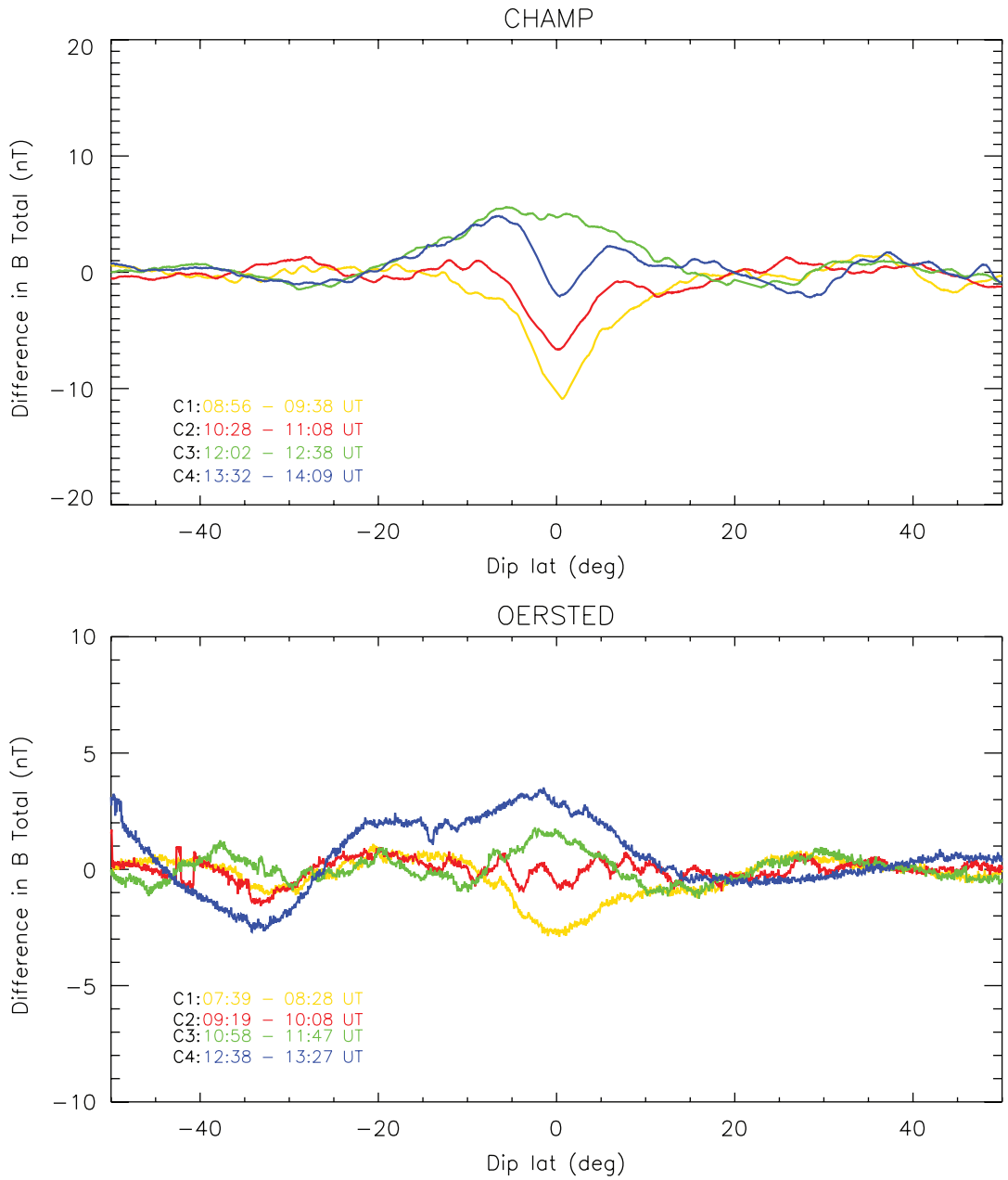

Fig. 6. 3 October 2005: Latitudinal variation of the total magnetic field component for CHAMP and Ørsted. Time of the different passes is indicated by color.

We have verified that the reversed magnetic signature of the electrojet at satellite altitude is caused by a CEJ and is not an artifact of data reduction. This data is supported by the switch in sign of the bipolar varying Z component (cf. Fig. 5), and by various comparisons with ground-based records during close-by overflights.

In the satellite observations two types of perturbed magnetic field variations are observed, as one can see for example, in passes B3 and B4 (CHAMP) (see Fig. 2). Pass B3 shows a reversal of the typical EEJ profile, with a positive maximum at the dip equator. This reflects the inversion of the magnetic field, and is therefore identified as a CEJ. Pass B4 also shows positive magnetic variations, which seem to be superimposed on the typical EEJ profile. This effect was previously detected in ground-based observations (Mayaud, 1977). The author suggested that the CEJ is superimposed on the EEJ throughout the day and that any strong attenuation of the H component (not necessary a full reversal) means that the CEJ is present. We would also like to point out that the satellite magnetic field measurements show in most cases a normal EEJ profile on the passes prior and/or during the eclipse while the passes after show the perturbed profiles or the CEJ profile. In some cases a clear evolution from a normal EEJ

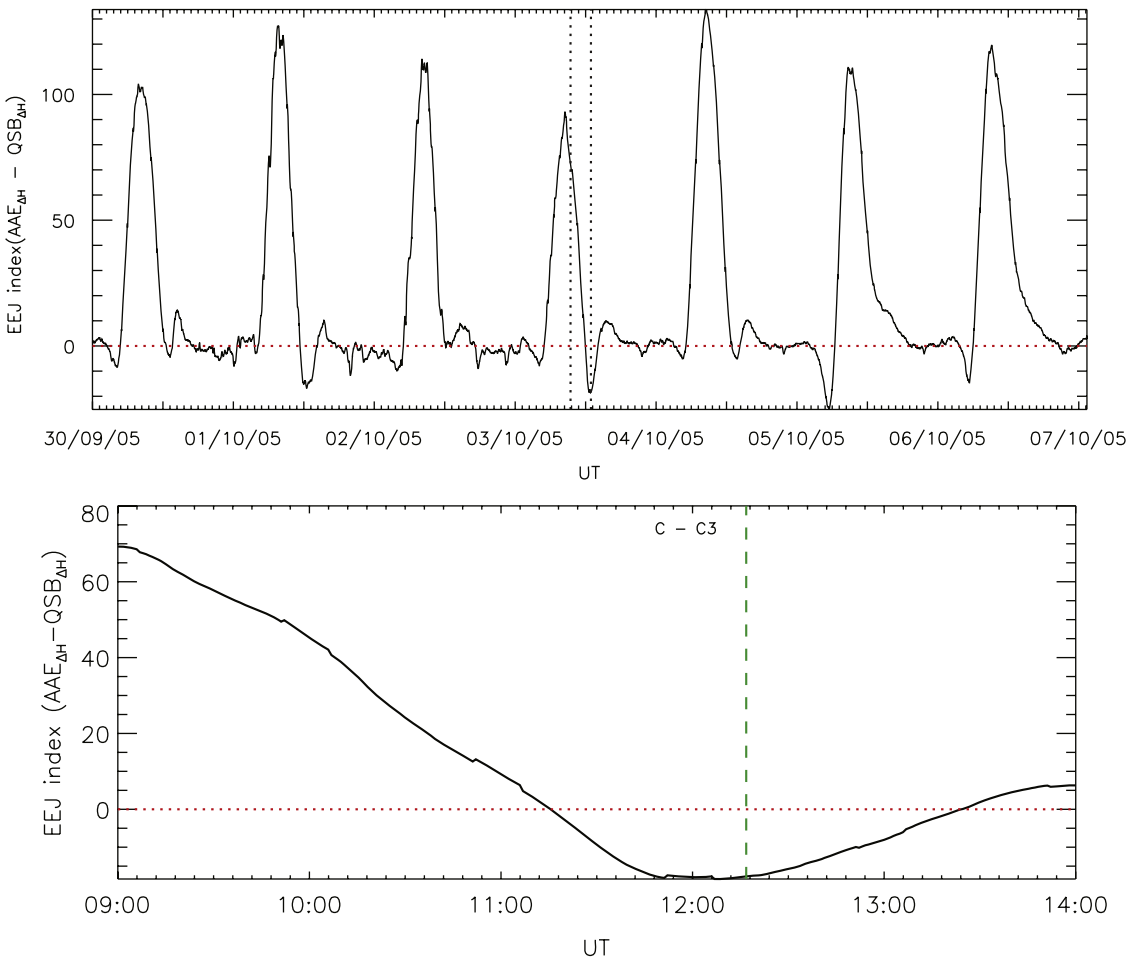

Fig. 7. Upper panel: EEJ index for the 30 September to 7 October 2005 period, obtained from the AAE/QSB stations. Vertical dotted lines indicate the eclipse period. Lower panel: EEJ index around the eclipse time. Dashed line indicates the CHAMP pass (C3) where a CEJ is observed.

to a reduced EEJ profile, followed by the CEJ is also seen. This systematic behavior in satellite observations makes it difficult to explain all the CEJ by pure incidence.

3.1. Spatio-temporal characteristics of the CEJ

In order to investigate more clearly if the observed effects are related to the eclipses we now try to derive the spatial and temporal characteristics of the electrojets. This task can be performed more efficiently if suitable ground- and space-based observations are available.

For the event on 10 June 2002 a good coverage is available. The observations at the YAP station reflect several negative turnings of the EEJ index during the eclipse period. We will not consider the negative excursions outside the period in the morning (~6 LT) and in the afternoon (~15 LT). The core shadow passed the dip equator in the morning at 7 LT close to YAP. Ørsted orbiting at a local time of 8:18 LT passes half an hour after (B2) and detects a clear CEJ, which is not seen in ground records. At that time the EEJ index is close to zero (cf. Fig. 3). About 20° further to the east a CEJ is detected by CHAMP (B3) at 00:37 UT, although an hour earlier SAC-C passed at a similar longitude but did not encounter a CEJ while the EEJ index was in both cases clearly negative. One should note, however, that a magnetic storm commenced around 10 UT of the 10th causing perturbations of the magnetic field (cf. Fig. 2). This could be primarily responsible for the CEJs recorded during that event.

Fig. 10, shows a spatio/temporal comparison of the Ørsted (B2) and of the B3 passes from the three satellites. In order to better visualize the differences between satellite derived magnetic fields the profiles have been scaled and their longitudinal extent is not accurately portrayed. This comparison suggests that the CEJ expanded eastward and covered at least the local time range from 9:40 to 11:12 LT at 00:30 UT. The CEJ lasted, with some interruptions, over the whole duration of the eclipse of about 3.5 h.

Another event with a good and conjugate ground/satellite coverage is the eclipse of 3 October 2005. The vicinity of the station AAE to the equator crossing of the eclipse makes it very suitable to monitor the temporal evolution of the related effects. At 11:15 UT, half an hour after the eclipse passage, the EEJ index turned negative. It lasted for more than 2 h until 13:25 UT. Right at the

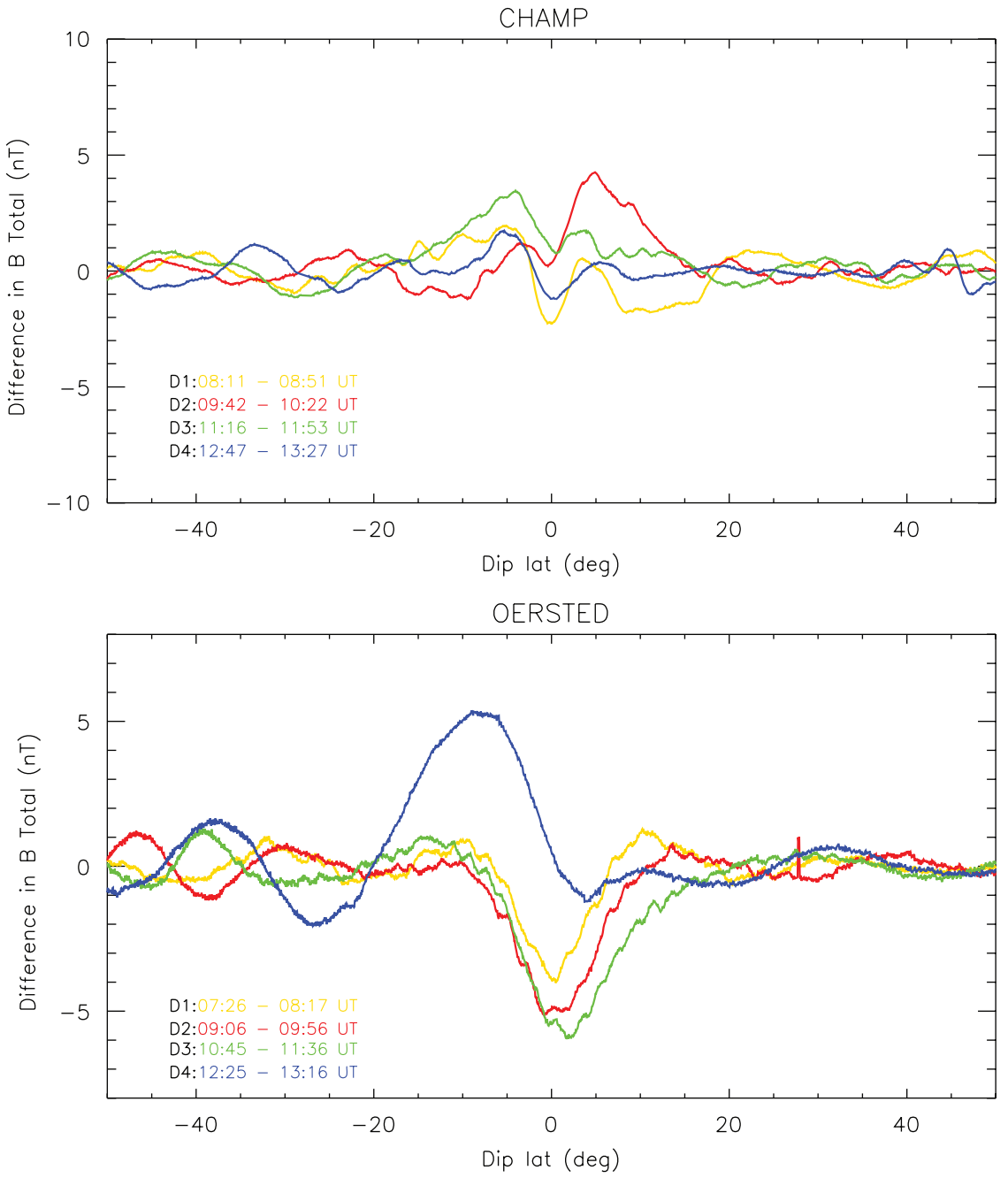

Fig. 8. 29 March 2006: Latitudinal variation of the total magnetic field component for CHAMP and Ørsted. Time of the different passes is indicated by color.

beginning of this interval Ørsted (C3) detected a weak CEJ 6° in longitude to the east of AAE. On its next orbit, 100 min later (C4), an even stronger CEJ is observed 18° to the west of AAE. CHAMP, crossing the dip equator at 12:17 UT (C3) about 100° to the west of AAE, also confirms the existence of a well-developed CEJ. This CHAMP pass coincides in time with the peak strength of the CEJ at AAE (cf. Fig. 7). We can conclude that CEJs existed at least around local times of 8:12 and 14:20 LT. There is unfortunately no concurrent observation of the EEJ in the noon sector. We should note, however, that two days before ground-based observations showed a CEJ at the same universal time which was not related to the eclipse, and we can therefore not exclude that CEJs tend to occur in this region in the morning sector and also around 14:30 UT, for other reasons.

For the remaining two events we cannot provide such a detailed description of the EEJ evolution. On 14 December 2001 CHAMP provided observations (A3) of a CEJ about 1.5 h after the eclipse crossing at a longitude 20° further

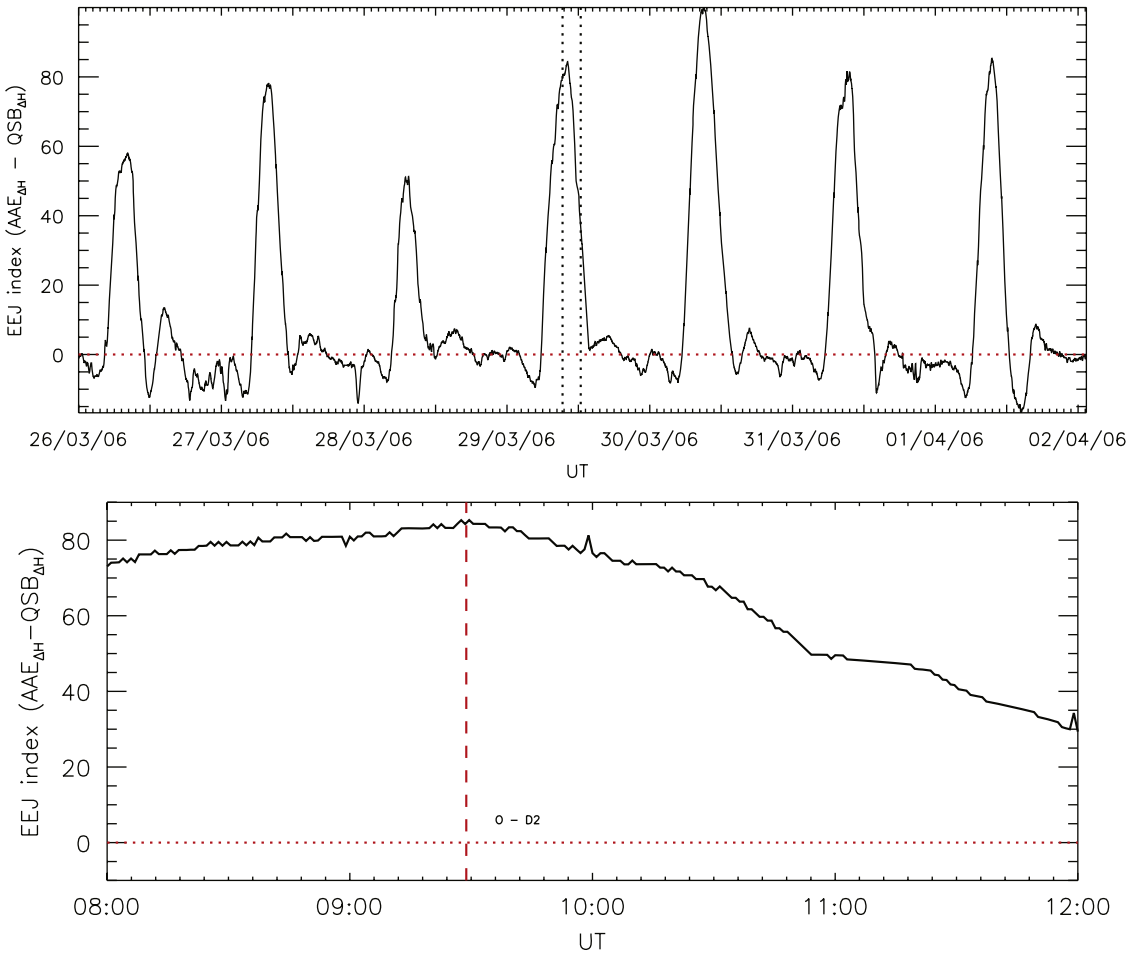

Fig. 9. Upper panel: EEJ index for the 26 March to 02 April 2006 period, obtained from the AAE/QSB stations. Vertical dotted lines indicate the eclipse period. Lower panel: EEJ index during the eclipse time. Dashed red line indicates the Ørsted pass (D2) closest to the AAE station.

east (cf. Fig. 4). On its subsequent passage CHAMP still found a CEJ close to the location of the eclipse crossing. To set an upper bound for the eastward end of the CEJ we looked at data from the Peruvian station HUA. This station about 50° to the east never recorded a CEJ on that day. The satellites Ørsted (11 LT) and SAC-C (10:30 LT) detected only some weak indications of westward currents on their A3 passes, 1 h after the eclipse, at a distance of about 40° to the west. When drawing on the results of the previously described events that the CEJ starts about half an hour after the eclipse has passed the dip equator and close to this location, we may conclude that the CEJ lasted at least 3 h and covered the local time range 12:30–15:30 LT.

The observational constellation for the eclipse on 29 March 2006 is also not too favorable. All recording sites are to the east of the crossing point. For example, AAE, about 30° to the east, shows no evidence of a significant eclipse effect (cf. Fig. 9). Even Ørsted passing only 3.5° to the east (D3), about 1.4 h after the eclipse (cf. Fig. 8), detected no indication of a deviation from a normal EEJ. Finally, on its last pass (D4) Ørsted measurements show evidence for some distorted westward flowing currents. This occurred 3.3 h after the eclipse crossing and 22° to the west. From this marginal observational evidence we cannot conclude that a CEJ formed as a consequence of the solar eclipse over the dip equator.

When summarizing the spatio-temporal evolution of the EEJ, observed at the time of eclipses, we can state that the intensity is reduced locally (cf. Fig. 7). The decrease is , however, not prominent, rather comparable with the day-to-day variability and can thus be masked by magnetic activity influences. In some cases CEJs tend to form about half an hour after the eclipse passed the dip equator and they last for 2–3 h. Spatially they extended either towards east or west. Similar to the occurrence during times not affected by eclipses, there seems to be a preference for an appearance away from noon. A typical longitudinal extent of 3 h in local time was found. In one case, 3 October 2005, there is observational evidence for concurrent CEJs at 8:10 and 14:50 LT.

3.2. *Dependencies and possible causes for the CEJ*

As we mentioned in the Introduction, the occurrence frequency of CEJ events seems to show a dependence on

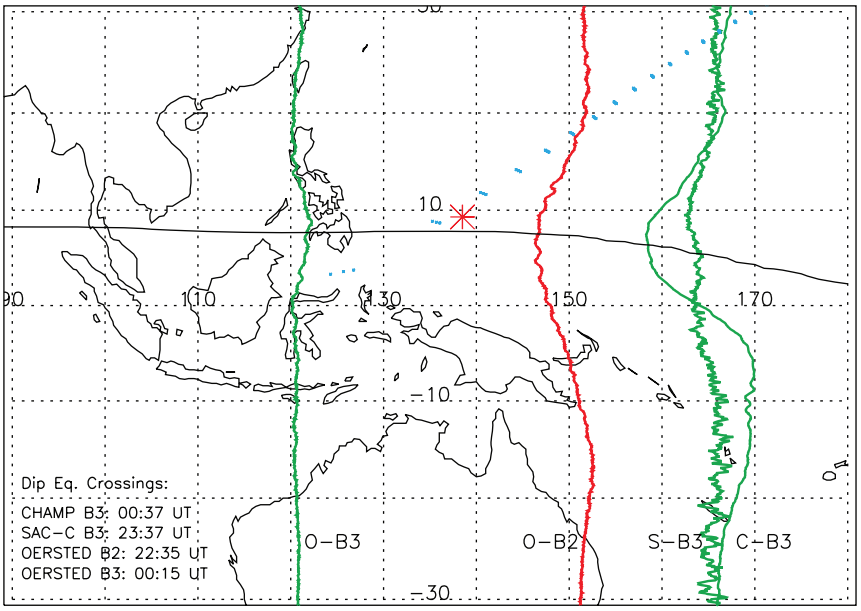

Fig. 10. Section of world map showing variation of the total magnetic field component during the 10 June 2002 eclipse, along the B2 pass of Ørsted (in red) and the B3 passes of the three satellites (in green). Cyan points indicate the eclipse path and the red star indicates the location of the YAP ground-based station. The universal time of the dip equator crossings is listed in the left corner.

four parameters: local time, season, solar activity and lunar phase. We can therefore compare the CEJ characteristics from our four eclipse events with respect to these parameters and relate them to previous observations. We should note that, as mentioned in the Introduction, a fifth event with a solar eclipse crossing of the dip equator, on 8 April 2005, was discussed in a previous paper by Tomás et al. (2007), but although a clear reduction of the EEJ strength was measured, no CEJ was observed. Detections of CEJs are presented here from nearly all longitudes, with the exception of a $\pm 15^{\circ}$ interval around the Greenwich meridian, from where no observations are available.

The CEJ occurrence was observed at different local times. Four detections were in the morning sector (CHAMP C3 and C4, Ørsted B1 and B2) and six in the afternoon sector (CHAMP A3, A4, D2 and D3), Ørsted C3 and C4). The remaining four CEJ observations were between 10:30 and 12:00 LT.

The five considered eclipses occurred in different seasons, two close to solstices and three close to equinoxes. The event with greatest number of CEJ detections by the three satellites occurred close to the June solstice (10 June 2002), but this event was strongly affected by the prevailing magnetic storm conditions. The December solstice event (14 December 2001) showed fewer but stronger CEJs. During equinox (3 October 2005) we observed clear CEJs in the morning and afternoon sectors. A very similar afternoon CEJ occurred, however, two days earlier. From the remaining two events we have only marginal or no evidence of CEJ.

In terms of solar activity our observations do not show a clear preference of CEJ for the low solar activity period, as claimed in previous works. The distribution of CEJs presented here does not follow that trend during high and moderate solar activity (14 December 2001 and 10 June 2002) as compared to low solar activity (8 April 2005, 3 October 2005 and 29 March 2006). Due to the small sample number this result cannot be considered significant.

All the eclipses occur by definition during new moon, and they are therefore in favor with CEJs observations, as mentioned by Mayaud (1977) and Rastogi (1989). The significance of the moon phase on the occurrence rate of the CEJ has; however, never been quantified.

The effects of solar eclipses on the EEJ have been addressed by Tomás et al. (2007). The authors report a strong reduction of the EEJ intensity in the wake of the eclipse. In this study we observe the occurrence of CEJs after the eclipse crossed the dip equator. Furthermore, the CEJ occurred always to the west of the eclipse location at the corresponding time, i.e. in the wake of the shadow zone. The occurrence of a CEJ can thus be a consequence of the reduction of the EEJ strength. This reduction is expected since due to the solar obscuration the conductivity diminishes and consequently so does the EEJ strength. In a recent study, Stolle et al. (2008) revealed from direct comparison between EEJ and vertical plasma drift measurements that there is on average a bias eastward electric field of 0.2 mV/m on top of the one driving the EEJ. As a consequence, CEJs up to −50 nT magnetic deflection are still accompanied by an eastward E-field. This implies that there is an additional westward current driven which dominates during times of weak EEJ.

All these suggestions should be checked in a dedicated study of the CEJ. Such a study should be based on various data sets obtained simultaneously from satellite, ground and radar facilities.

In summary, this study focused on the identification of typical solar eclipse effects on the EEJ. We find that the EEJ is locally depressed, but the reduction is comparable to the day-to-day variability. In four out of five cases the formation of a CEJ could be observed. The CEJ forms about 1 h after the core shadow passed the dip equator and it lasts for 2–3 h. The location of the CEJ is always westward, in the wake of the eclipse. Based on this relative spacing between the two phenomena we prefer the explanation that the primary cause for the CEJs is the depression of the EEJ by the eclipse. The number of observed events is too small for making firm statements on the relation between solar eclipses and CEJs.

Acknowledgments

The authors would like to thank M. Rother for his help in processing the magnetometer data. The operational support of the CHAMP mission by the German Aerospace Center (DLR) and the financial support for the data processing by the Federal Ministry of Education and Research (BMBF) are gratefully acknowledged. The work of A.T. Tomás is financed by a DFG (Deutsche Forschungsgemeinschaft) Research Fellowship.

References

Beynon, W.J.G., Brown, G.M., 1956. Solar eclipses and the ionosphere. Journal of Atmospherical and Terrestrial Physics 6 (Special Suppl.).

Cheng, K., Huang, Y.-N., Chen, S.-W., 1992. Ionospheric effects of the solar eclipse of September 23, 1987, around the equatorial anomaly crest region. Journal of Geophysical Research 97, 103–111.

Forbes, J., 1981. The Equatorial electrojet. Reviews of Geophysics and Space Physics 19 (3), 469–504.

Korte, M., Lühr, H., Förster, M., Haak, V., 2001. Did the solar eclipse of August 11, 1999, show a geomagnetic effect. Journal of Geophysical Research 106 (A9), 18563.

Maus, S., Rother, M., Stolle, C., Mai, W., Choi, S., Lühr, H., Cooke, D., Roth, C., 2006. Third generation of the Potsdam magnetic model of the Earth (POMME). Geochemistry Geophysics Geosystems 7, Q07008.

Mayaud, P.N., 1977. The equatorial counter electrojet—a review of its geomagnetic aspects. Journal of Atmospheric and Terrestrial Physics 39, 1055–1070.

Neubert, T., Mandea, M., Hulot, G., von Frese, R., Primdahl, F., Jørgensen, J.L., Friis-Christensen, E., Stauning, P., Olsen, N., Risbo, T., 2001. Ørsted satellite captures high-precision geomagnetic field data. Eos Transactions AGU 82 (7), 81–81.

Olsen, N., Lühr, H., Sabaka, T.J., Mandea, M., Rother, M., Tøffner-Clausen, L., Choi, S., 2006. CHAOS—A model of the Earth's magnetic field derived from CHAMP, Ørsted, and SAC-C magnetic satellite data. Geophysical Journal International 166 (1), 6775.

Onwumechili, C.A., 1997. The Equatorial Electrojet. Gordon and Breach Science Publishers, Amsterdam, Netherlands.

Rastogi, R.G., 1974. Westward equatorial electrojet during daytime hours. Journal of Geophysical Research 79 (10), 1503–1512.

Rastogi, R.G., 1989. The equatorial electrojet: magnetic and ionospheric effects. In: Jacobs, J. (Ed.), Geomagnetism, vol. 3. Academic Press, San Diego, CA, pp. 1503–1512.

Reddy, C.A., 1989. The equatorial electrojet. In: Campbell, W.H. (Ed.), Quiet Daily Geomagnetic Fields, vol. 131 no. 3. Birkhäuser, Basel Germany, pp. 485–508.

Reigber, C., Lühr, H., Schwintzer, P., 2002. CHAMP mission status. Advances in Space Research 30 (2), 129–134.

Rishbeth, H., 2000. The equatorial F-layer: progress and puzzles. Annalles Geophysicae 18, 730–739.

Salah, J.E., Oliver, W.L., Foster, J.C., Holt, J.M., 1986. Observations of the May 30, 1984, annular solar eclipse at Millstone Hill. Journal of Geophysical Research 91 (A2), 1651–1660.

Somayajulu, V.V., Cherian, L., Rajeev, K., Ramkumar, G., Reddi, C.R., 1993. Mean winds and tidal components during counter electrojet events. Geophysical Research Letters 20 (14), 1443–1446.

Stolle, C., Manoj, C., Lühr, H., Maus, S., Alken, P., 2008. Estimating the day time equatorial ionization anomaly strength from electric field proxies. Journal of Geophysical Research in press.

Tomás, A.T., Lühr, H., Förster, M., Rentz, S., Rother, M., 2007. Observations of the low latitude solar eclipse on 8 April 2005 by CHAMP. Journal of Geophysical Research 112, A06303.